THE RELATION BETWEEN DISTRIBUTION OF HUMIDITY AND TYPES OF RAINFALL ON THREE RAINBANDS NEAR SHANGHAI DURING MEIYU PERIOD IN 2001.

*Shingo Shimizu[1)], Hiroshi Uyeda[1)], Taro Shinoda[1)],Kazuhisa Tsuboki[1)], Hiroyuki Yamada[2)], Biao Geng[2)]

[1)]Hydrospheric Atmospheric Research Center, Nagoya University

[2)]Frontier Observational Research System for Global Change

1. Introduction

In a moist environment as Asian monsoon region, the relation between environment and types of rainbands has not been documented well. In a dry environment as the Great Plains, convective available potential energy (CAPE) and vertical wind shear are important environmental parameters for determining formation types of rainbands (Bluestein and Jain, 1985; Bluestein and Marx, 1987). In a moist environment, a humidity distribution, as well as CAPE and vertical wind shear, is focussed as an important parameter for maintenance of supercell (Shimizu et al., 2001). In this study, we investigate the role of the humidity distribution on the maintenance of convective cells in a rainband, and propose the environmental parameters for distinguishing formation types of rainbands and for determining the rainfall types.

Three distinct types of rainbands with heavy rainfall were observed near Shanghai in 2001 (CASE1: 24 June, CASE2: 19 June, CASE3: 6 July). We investigated the structures and formation types of three rainbands by dual Doppler radar analyses and estimated environmental parameters around the rainbands with Regional objective analysis (RANAL) data produced by the Japan Meteorology Agency.

2. Data and analysis method

Two X-band Doppler radars (at Wuxian and Zhouzhuang, covering the downstream of the Changjiang river with 64 km in radius) obtained sets of volume scan data of reflectivity and Doppler velocity every six minutes. We analyzed three dimensional structure of the rainbands by using dual Doppler analysis for the overlapped observation area of the two radars (Fig. 1).

In order to evaluate the environment around the observation area, we divided the 4° × 4° re-

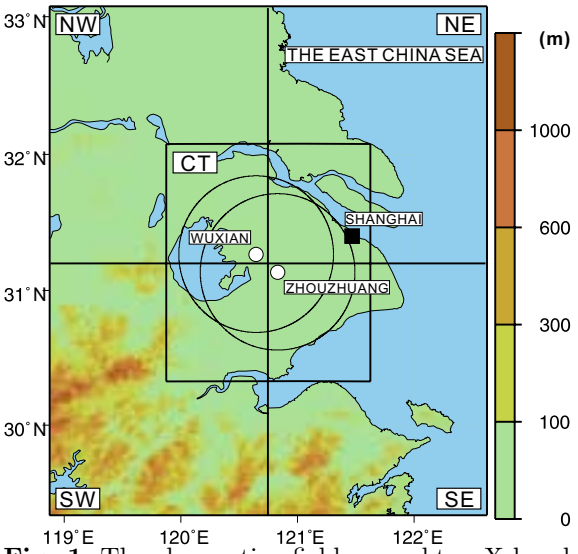

Fig. 1: The observation field around two X-band Doppler radars at Wuxian and Zhouzhuang. Five of 2°×2° regions (NW,NE,SW,SE, and CT) indicate analysis regions for estimating environmental parameters (Table 1) using RANAL.

Table 1: Definitions of six environmental parameters estimated by using RANAL data.

$$CAPE = -R\int_{p_{LFC}}^{p_{top}} (T_p - T_e)\, d(\ln p)$$

$$CIN = -R\int_{p_{base}}^{p_{LFC}} (T_p - T_e)\, d(\ln p)$$

$$VISH = -\frac{1}{g}\int_{surf}^{850hPa} q\, dp$$

$$HUDE = -\frac{1}{g}\int_{850hPa}^{500hPa} (q_s - q)\, dp$$

$$VWS = \frac{1}{H}(Mean\vec{V}_{surf-6km} - Mean\vec{V}_{surf-500m})$$

$$VFC = -div(-\frac{1}{g}\int_{surf}^{850hPa} q\vec{V} dp)$$

T_e :temperature of environment H :height(=2.5 km)
T_p :temperature of parcel $\vec{V}$:wind vector
q :specific humidity q_s :saturated specific humidity
$Mean\vec{V}_{surf-6km}$:mean wind from surface to 6 km ASL
$Mean\vec{V}_{surf-500m}$:mean wind from surface to 500 m ASL

* Corresponding author address: Shingo Shimizu, Hydrospheric Atmospheric Research Center, Nagoya University, Nagoya 464-8601, Japan
Email: shimizu@rain.ihas.nagoya-u.ac.jp

gion (depicted in Fig. 1) into four regions (2°×2° quadrants centering at the two radars) named as NE, NW, SE, SW. We added 2°×2° region named as CT just over the observation area. We investigated the each environment in the five regions using RANAL data.

The time resolution of the RANAL is 6 hours (02, 08, 14, 20 LST). The horizontal resolution of the RANAL is 20 km. In the vertical direction, the RANAL contains 20 levels.

The mean of six environmental parameters (Table 1) in the each region are calculated: Vertical wind shear between mean wind from surface to at a height of 6 km above sea level (ASL) and mean wind from surface to 500 m ASL (VWS), the CAPE, vertical integrated specific humidity from surface to 850 hPa (VISH), vertical integrated specific humidity deficit from 850 hPa to 500 hPa (HUDE), and vertical integrated vapor flux convergence from surface to 850 hPa (VFC). For accurate calculation of these parameters, in this study, we converted the vertical 20 levels data to 211 levels data (5 hPa interval) by linear interpolation.

The VISH and the HUDE are indices wetness of lower layer, and for dryness of midlevel layer, respectively.

3. Characteristics of three rainbands

In order to reveal different types of formation and rainfall among three rainbands (CASE1: 0400 local standard time (LST)* 24 June, CASE2: 0118 LST 19 June, CASE3: 1706 LST 6 July), developing near Shanghai during Meiyu period in 2001, we investigate radar reflectivity fields of the three cases at 1.0 km ASL in Fig. 2. The strong echo over 35 dBZe in CASE1 and CASE2 had line shape, while that of CASE3 corresponded to discrete convective cells.

In CASE1, strong echo over 30 dBZe to the south of the rainband developed and merged with the rainband after 0406 LST. In this way, in CASE1 and CASE2, a new convective cell developed continually to the southwest of the rainband, and merged with the rainband. On the contrary, in CASE3, the discrete convective cells developed and merged with each other, and formed the line shape. Rainbands of CASE1 and CASE2 had characteristics of back-building type, a rainband of CASE3 had characteristics of broken type (Bluestein and Jain, 1985).

*LST = UTC + 8 hours

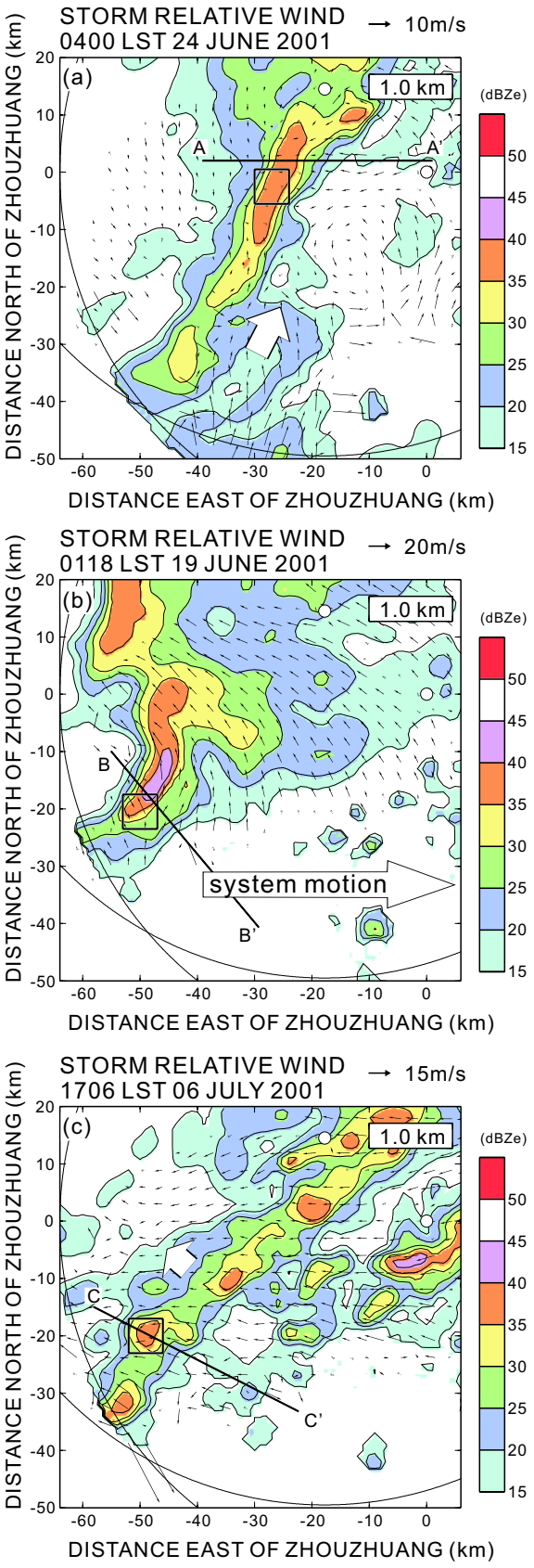

Fig. 2: Radar reflectivity overlaid with storm-relative wind vectors at 1 km ASL of CASE1 (a), CASE2 (b), and CASE3 (c). Open arrows indicate system propagation speed and the direction. Squares indicate analysis areas for vertical profiles in Fig. 3. Vertical cross sections along A-A', B-B', and C-C' line are indicated in Fig. 5.

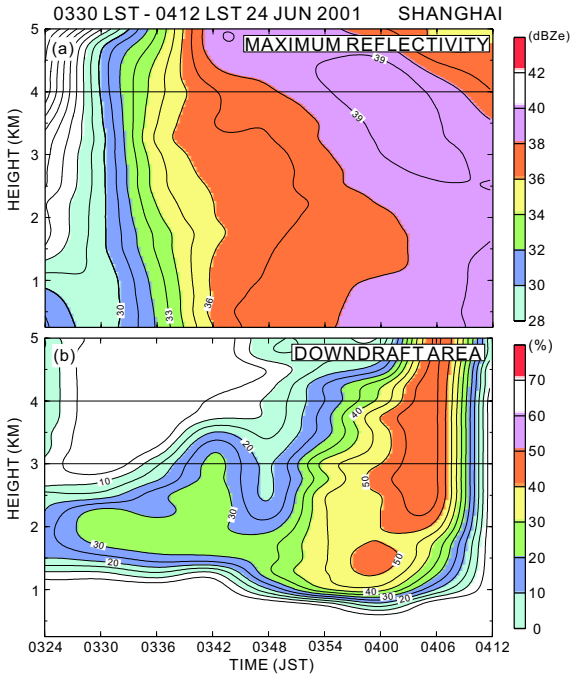

Fig. 3: Time-height cross sections of the maximum reflectivity (a) and the ratio of downdraft area to the area which has vertical wind velocity (b) on CASE1.

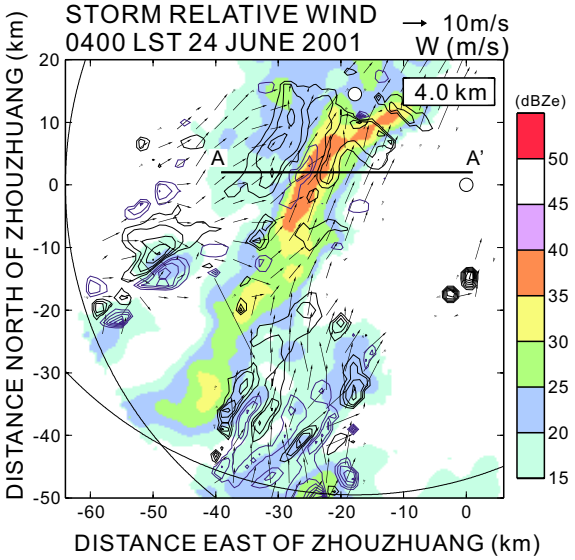

Fig. 4: Reflectivity fields overlaid with storm-relative wind vectors at 4 km ASL in CASE1. Solid and blue contours indicate updraft and downdraft velocity, respectively (every 1 $m\ s^{-1}$).

With regard to flow structure at 1.0 km ASL (Fig. 2), storm-relative inflow in CASE1, CASE2, and CASE3 came from east-southeast, south-southwest, and southeast, respectively.

The mean propagation speed and direction in CASE1, CASE2, and CASE3, indicated by open arrow in Fig. 2, were 2.4 m s^{-1} northeastward, 13.0 m s^{-1} eastward, and 1.4 m s^{-1} northwestward, respectively.

In order to characterize the different types of rainfall, we focussed on lifetime of a convective cell in the rainbands. Squares in Fig. 2 indicate analysis areas (6 km $\times$ 6 km) for vertical profiles in Fig. 4. We chased the analysis areas which contain the updraft core and downdraft core of a convective cell. We investigated time series of the maximum reflectivity and the ratio of downdraft area to the area which has vertical wind within the analysis areas.

We defined lifetime of convective cell as following. The time, when the maximum reflectivity over 30 dBZe reached at 4 km ASL, is defined as a start of mature stage of convective cell. The time, when the downdraft area between 3 km ASL and 4 km ASL have a peak, and the updraft core at 1 km ASL disappear, is defined as an end of dissipating stage. Convective cells of CASE1 were long-lived (42 minutes: 0330 LST - 0412 LST) in Fig. 3, while those of CASE2 and CASE3 were short-lived (30 minutes: 0106 LST - 0136 LST, 1654 LST - 1724 LST) (not shown). The rainband of CASE1 had steady structure, because the rainband was maintained by the steady convective cell. On the contrary, the rainbands in CASE2 and CASE3 are maintained by repeated replacement of the convective cells.

As depicted in Fig. 3, the lifetime of convective cell depends on the peak of downdraft around 4 km ASL. We investigate the cause of the strengthening of the downdraft at 4 km ASL in Fig. 4 and Fig. 5. The reflectivity overlaid with storm-relative wind at 4 km ASL, and vertical wind velocity in CASE1 are shown in Fig. 4. The downdraft core at 4 km ASL located where the southwesterly wind blew into strong echo core.

In CASE2, the northwesterly and southwesterly wind at 4 km ASL blew into strong echo. In CASE3, the northwesterly wind blew into strong echo (not shown). The downdraft core in CASE2 and CASE3 also located at the confluence of the wind and the edge of strong echo.

Vertical cross sections along the A-A', B-B', and C-C' lines in Fig.2 are shown in Fig. 5. The maximum updraft velocity at 4 km ASL in CASE1, CASE2, and CASE3 was 2.0 m s^{-1}, 14.0 m s^{-1}, and 5.0 m s^{-1}, respectively. The maximum downdraft velocity at 4 km ASL in CASE1, CASE2, and CASE3 was 3.0 $m\ s^{-1}$, 12.0 $m\ s^{-1}$, and 4.0 $m\ s^{-1}$, respectively. The location of downdraft

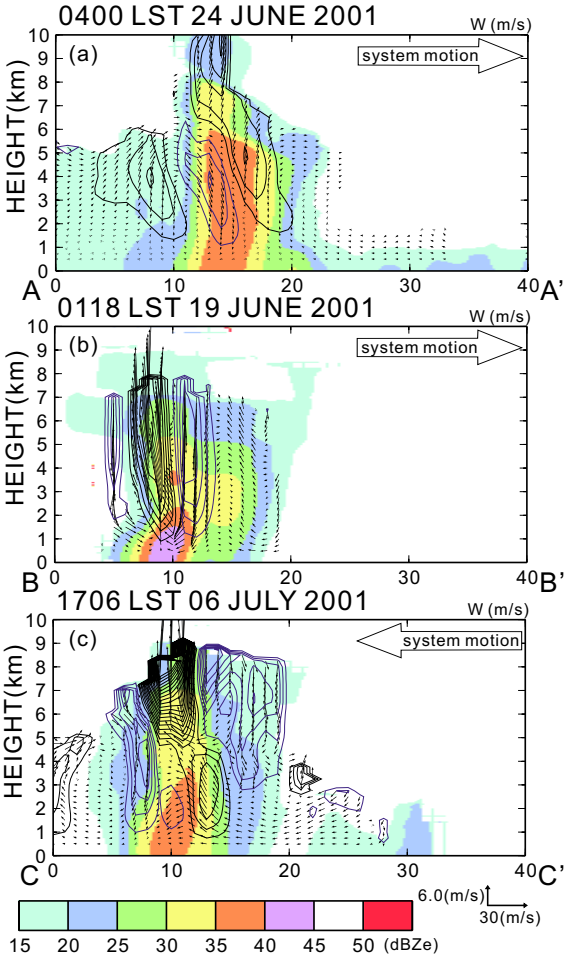

Fig. 5: Vertical cross sections along A-A', B-B',and C-C' lines in Fig. 2 on CASE1 (a), CASE2 (b), and CASE3 (c). Solid and blue contours indicate updraft and downdraft velocity every 1 $m\ s^{-1}$ except for CASE2 (every 3 $m\ s^{-1}$), respectively.

core differed from the location of the reflectivity core in all cases.

The cause of downdraft seems to be mainly due to evaporative cooling in all cases because the downdraft core located at the edge of strong echo region in all cases (Fig. 5). We investigate which environmental parameters determine the efficiency of evaporative cooling in next section.

4. Environments of three rainbands

We investigate the environment a few hours before the development of the three rainbands, in order to find useful environmental parameters to distinguish types of rainband before it develops, and to understand the development mechanism of rainbands in a moist environment.

The distribution of the CAPE and the CIN of CASE1 is indicated in Fig. 6. The CIN is distributed over the ocean, while the CAPE is distributed over the mountains. Vapor flux vectors in Fig. 6 indicate that plenty of vapor was supplied from the ocean to the land. The CIN over the ocean restrained vertical transport of vapor, thus abundant vapor was horizontally transported from ocean to the observation area. The mean value of the VFC in the CT region was over -6.95 $\times$ 10^4 kg m^{-1} s^{-1}. This abundant vapor was transported over the radar site and supplied to the rainband.

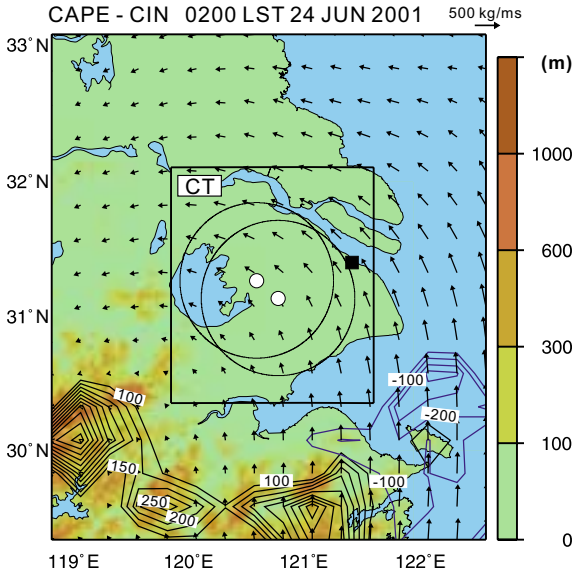

Fig. 6: The distribution of the CAPE (solid contour) and the CIN(blue contour). The contour interval is 50 $J\ kg^{-1}$ (starting $\pm$ 100 $J\ kg^{-1}$). Vectors indicate vapor flux integrated from surface to 850 hPa.

The distribution of the HUDE overlaid with wind at 4 km ASL are shown in Fig. 7. The moist air (the HUDE was less than 2 kg m^{-2}) existed over the observation area, while the dry air existed over the ocean. The wind at 4 km ASL blew from the very moist SW region.

In order to evaluate the environment quantitatively, and to compare three cases, we calculated the mean value of the six environmental parameters in five regions. We select a region from five regions by following rules. The mean value of the CAPE, and the CIN are selected in the region where the rainband developed. The mean value of VISH (the HUDE) is selected in the region which the storm-relative wind at 1 km (4 km) ASL blew from. The VDF and the VWS are calculated only in CT region. The values of these parameters are shown in Table 2. We compare the values of six environmental parameters of the three cases.

In CASE1, the value of CAPE was the lowest of the three. This low value of CAPE led to the

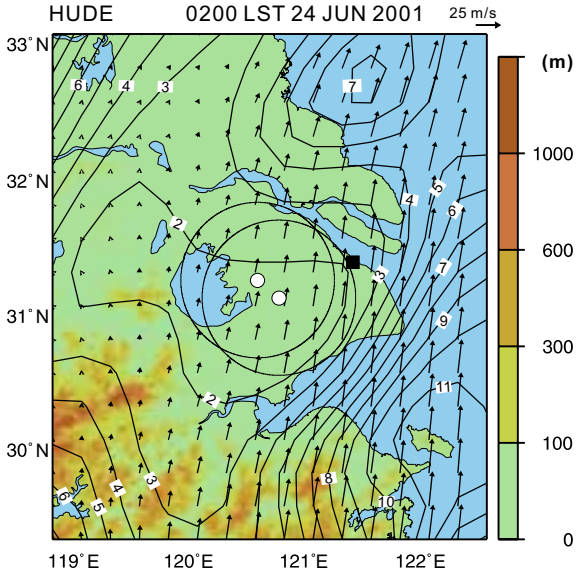

Fig. 7: The distribution of the HUDE and wind at 4 km ASL. The contour interval is 1 kg m^{-2}.

weakest updraft velocity. Plenty of vapor existed in lower layer because the VISH had large value, in addition, an abundant vapor is accumulated at lower layer because the VFC had the highest value. This abundant vapor converted into abundant rain by updraft. However, because of the lowest value of the HUDE, the abundant rain could not evaporate. Therefore, the downdraft velocity in Fig. 5a was the weakest.

In CASE2, the HUDE had the highest value, and the CAPE had also the highest value. In addition, the value of VFC was large value. Thus, the efficiency of evaporative cooling was the largest because abundant lower vapor was transported to the driest midlevel layer. Therefore, the downdraft in CASE2 was the largest in Fig. 5b.

In CASE3, the HUDE and VISH had high value, however the CAPE and VDF had small value. A abundant vapor existed in lower layer, however vertical transportation of rain was so small that the downdraft was not strong in Fig. 5c.

The evaporatively cooled downdraft strength is well explained by the HUDE, and the combination of the CAPE, the VISH, and the VFC. We investigate the relation of the downdraft strength and the VWS and lifetime of convective cells.

The mean of the VWS in the CT region is indicated in Table 2. In CASE3, the small value of VWS led to the short-lived convective cell, because precipitation forms within the updraft and produces negative buoyancy that destroys the convection.

In CASE2, the VWS had large value, but the strong downdraft caused short-lived cells, because the strong downdraft led to strong low-level outflow, it undercuts the warm inflow into the updraft thereby weakens the convective cell. In CASE1, the convective cell was long-lived.

We revealed that combination of the six parameters determined the downdraft strength and lifetime of convective cells within the rainbands.

5. Discussion

We described the formation and rainfall types of the rainbands in Section 3, and revealed that the relation between the characteristics of convective cells within rainbands and the environment in Section 4. In this section, we discuss the relation between the characteristics of the convective cell and rainfall type of rainbands.

Bluestein and Jain (1985) revealed that high value of CAPE (mean value: 2090 J kg^{-1}) and high value of vertical wind shear (mean value: 4.8×10^{-3} s^{-1}, from surface to 6 km ASL) are suitable condition for the line formation of back-building type, while high value of CAPE (mean value: 2820 J kg^{-1}) and low value of vertical shear(mean value: 3.3×10^{-3} s^{-1}, from surface to 6 km ASL) lead to the line formation of broken type.

In this study, when the vertical wind shear was small such as CASE3, the formation of the rainband was broken type, when the vertical wind shear was large such as CASE1, CASE2, the formation of the rainband was back building type. However, the value of CAPE in all cases was much smaller than that of Bluestein and Jain (1985). In a moist environment, even if CAPE is very small such as CASE1, the high value of VFC substitutes the CAPE for development of rainbands with heavy rain.

For the formation of back-building lines in a moist environment, the large vertical wind shear is essential condition as well as in a dry environment, however high value of CAPE is not indispensable condition. In other words, a strong updraft is not always necessary element for the formation of back building type. Instead of the CAPE, the high value of VFC is an indicator of vertical transportation of vapor with weak updraft (such as CASE1). In addition to the CAPE and VWS, we propose the VFC as useful parameter to distinguish formation type. The more statistical studies on the formation types of rainbands focusing on the VFC, CAPE, and VWS would verify our proposition,

and determine the threshold value of the VFC, CAPE, and VWS.

We need to reveal not only the relation between the environment and formation types of rainbands, but also the relation between the environment and types of rainfall. Because the rainbands of CASE1 and CASE2 had same formation type, however the rainfall types of the two rainbands were very different. The rainband of CASE2 caused heavy rainfall and severe downburst with fast propagation, while CASE1 caused steady rainfall and weak downdraft with slow propagation.

We revealed that the HUDE and the combination of the VFC, the VISH, and the CAPE determine the downdraft strength in Section 4. The combination of the downdraft strength and the VWS is useful to predict the steadiness and propagation speed of rainbands. This characteristics of rainbands (steadiness and propagation speed) determine the rainfall type.

The research on environmental parameters reflected in humidity distribution (such as the HUDE or the VFC) give us strong possibility to predict rainfall type for preventing disaster and to understand the development mechanism of rainbands in a moist environment.

6. Conclusions

We investigated the humidity distribution for distinguishing the formation types of rainbands and rainfall types on three rainbands developing near Shanghai during Meiyu period in 2001.

We revealed that the dryness of midlevel (the HUDE) and amount of vapor supplied from lower layer (the combination of the VFC, the CAPE, the VISH) decide whether a rainband causes intensive rain for short time or continuous rain for long time.

For distinguishing the formation types of rainbands in a moist environment, as well as the buoyancy and vertical shear, we proposed to focus on the vapor flux convergence in lower layer.

More case studies and statistically studies on rainbands in a moist environment with focusing on humidity distribution would lead to more accurate prediction of heavy rainfall for preventing disaster, and a clear understanding of the rainbands in a moist environment.

REFERENCES

Bluestein, H. B. and M. H. Jain, 1985: Formation of Mesoscale Lines of Precipitation: Severe Squall Lines in Oklahoma during the Spring. *J. Atmos. Sci.*, **42**, 1711–1733.

Bluestein, H. B. and G. T. Marx, 1987: Formation of Mesoscale Lines of Precipitation: Nonsevere Squall Lines in Oklahoma during the Spring. *Mon. Wea. Rev.*, **115**, 2719–2727.

Shimizu, S., H. Uyeda, Q. Moteki, T. Maesaka, Y. Takaya, K. Akaeda, T. Kato and M. Yoshizaki, 2001: Maintenance mechanism of a 24 May 2000 supercell storm developing in moist environment over the Kanto Plain, Japan. *International Conference on Mesoscale Meteorology and Typhoon in East Asia*, 30–35.

Table 2: Characteristics and schematic models of three rain bands and environmental parameters.

	CASE1	CASE2	CASE3
LINE TYPE	steady Back-building line	Back-building Line	Broken Line
Maximum downdraft(at 4km) [m/s]	3.0	12.0	4.0
Propagation speed [m/s]	2.4	13.0	1.4
VWS [1/s ×10*-3]	2.60	3.88	0.34
CAPE [J/kg]	78.6	1646	323.9
VISH [kg/m*2]	24.1	18.5	26.4
HUDE [kg/m*2]	3.14	9.99	7.57
VFC [kg/(ms)×10*4]	6.95	3.66	1.02
Schematic model Echo structure at 1km Downdraft core at 4 km Downdraft core at 1 km System-relative wind at 4 km System-relative wind at 1 km